CHEMCATCHEM

DOI: 10.1002/cctc.201100027

Mechanism and Site Requirements of Thiophene Hydrodesulfurization Catalyzed by Supported Pt Clusters

Huamin Wang and Enrique Iglesia*[a]

Kinetic, isotopic, and chemical analysis methods are used to examine the identity and kinetic relevance of elementary steps and the effects of Pt cluster size on thiophene hydrodesulfurization (HDS) turnover rates. Quasi-equilibrated H_2 and H_2S heterolytic dissociation steps lead to sulfur chemical potentials given by the prevalent H_2S/H_2 ratio and to cluster surfaces with a metallic bulk, but near-saturation sulfur coverages, during steady-state catalysis. Sulfur-vacancies on such surfaces are required for η^1(S) or η^4 thiophene adsorption modes and for H_2 and H_2S dissociation steps. H-assisted C–S bond cleavage of η^1(S) thiophene and H-addition to η^4 thiophene limits rates of direct desulfurization and hydrogenation sulfur removal pathways, respectively. These steps, their kinetic relevance, and the prevalent sulfur-saturated surfaces resemble those on Ru clusters; they are also consistent with the observed kinetic effects of reactants and products on rates, with the rapid isotopic exchange in $H_2/D_2/H_2S$ mixtures during HDS catalysis, and with measured H_2/D_2 kinetic isotope effects. Small Pt clusters exhibit lower turnover rates, stronger inhibition by H_2S, and a greater preference for desulfurization pathways than those of large clusters. These effects reflect the prevalence of coordinatively unsaturated corner and edge sites on small clusters, which bind sulfur atoms more strongly and lead to lower densities of vacancies and to a preference for η^1(*S*)-bound thiophene species. Sulfur binding energies and their concomitant effects on the number of available vacancies also account for the higher turnover rates measured on Pt clusters compared with Ru clusters of similar size. These data and their mechanistic interpretation suggest that the concepts and steps proposed here apply generally to hydrogenation and direct desulfurization of organosulfur compounds. Taken together with similar observed effects of oxygen binding strength, metal identity, and cluster size for oxidation reactions of NO, hydrocarbons, and oxygenates, which also require vacancies in their respective kinetically relevant steps, these data also indicate that low reactivity of small clusters may reflect in most instances their coordinative unsaturation and the concomitant kinetic and thermodynamic preference for low vacancy concentrations on nearly saturated surfaces.

Introduction

Hydrodesulfurization (HDS) processes remove sulfur atoms from hydrocarbons by chemical reduction to hydrogen sulfide using H_2 with transition metals and their sulfides as catalysts. Mechanistic and structural insights, concerning reaction pathways and catalysts, respectively, are required to design more effective HDS catalysts, with higher rates at lower H_2 pressures, so as to meet emerging requirements for ultra-low sulfur fuels without excessive costs.[1–5] Extensive studies of HDS pathways and site requirements have been performed on commercial Co(Ni)Mo(W) sulfide compositions.[1–11] Nevertheless, the atomic structure of active sites and its consequences for surface reactivity remain controversial, to some extent because of challenges in establishing the number and type of surface structures in non-uniform and anisotropic Co(Ni)Mo(W) sulfides with lamellar structures.[12]

Other transition metals and their sulfides are also active HDS catalysts[1,5,13–23] and the observed periodic trends have led to several proposals for electronic and sulfur binding energy effects as descriptors of HDS reactivity and selectivity.[1,8,13,16,18–23] Some reports suggest an inverse relation between intrinsic reactivity and metal–sulfur bond energies in the corresponding sulfides,[18,19] while others report a volcano-type dependence with maximum rates at intermediate metal–sulfur bond energies.[8,13,20–23] These conclusions are supported by rates only occasionally measured as turnover rates on materials of uncertain bulk structure and phase during catalysis, and at conditions and sulfur chemical potentials that led to significant axial gradients in reactivity, sulfur coverages, and even thermodynamically stable phases.

Here, we report the intrinsic reactivity of supported Pt clusters in HDS reactions, provide a rigorous mechanistic interpretation for these properties from kinetic and isotopic data, and contrast the behavior of Pt clusters with that of Ru-based materials.[17] Pt and Ru are among the most active HDS catalysts[1,5,13–23] and form well-defined isotropic structures as both metals and sulfides; as a result, they are more amenable to structural and functional assessment by experiment and theory. Our recent studies have shown that Ru clusters are

---

[a] *Dr. H. Wang, Prof. E. Iglesia*
Chemical Sciences Division, Lawrence Berkeley National Laboratory
and Department of Chemical Engineering
University of California, Berkeley, CA 94720 (USA)
Fax: (+1) 510-642-4778
E-mail: iglesia@berkeley.edu

Supporting information for this article is available on the WWW under http://dx.doi.org/10.1002/cctc.201100027.

present as metal clusters with sulfur-saturated surfaces during HDS catalysis and that sulfur vacancies are required for kinetically relevant steps in both parallel hydrogenation and desulfurization HDS paths at temperatures, pressures, and H_2S levels relevant to the practice of HDS catalysis.[17] HDS occurs by means of parallel hydrogenation (HYD) and direct desulfurization (DS) routes; turnover rates for both routes decreased with decreasing Ru-cluster size because the stronger sulfur binding at the surfaces of small clusters decreases the concentration of the required sulfur vacancies during steady-state HDS catalysis. The sulfur binding strength at the metal surfaces also depends strongly on metal identity,[24] however, rigorous correlations between the metal–sulfur bond energies and turnover rates for metals that do not form bulk sulfides at practical HDS conditions are, to our knowledge, not available. Recent studies on the oxidation reactions of dimethyl ether[25] and NO,[26,27] which also require vacancies on oxygen saturated metal surfaces in their respective kinetically relevant steps, have shown that Pt clusters give higher turnover rates than Pd or Rh clusters, as a consequence of the concomitant trends in metal–oxygen bond energies and the prevalent concentration of oxygen vacancies.[25–27]

Here, we report thiophene turnover rates and selectivities at conditions relevant to HDS practice on Pt clusters with a wide range of metal dispersion (0.13–0.81 nm and 1.4–8.4 nm mean diameter) on inert SiO_2 supports. Small Pt clusters show lower hydrogenation and desulfurization turnover rates, because of stronger metal–sulfur bonds at coordinatively unsaturated corner and edge sites, which are prevalent on small metal clusters, and concomitantly lower vacancy concentrations during steady-state catalysis. Weaker metal–sulfur bonds and higher vacancy concentrations lead to higher turnover rates on Pt than on Ru clusters of a given size. Kinetic and isotopic data are consistent with the essential role of sulfur vacancies in hydrogenation and desulfurization pathways and with a sequence of elementary steps similar to that involved in HDS reactions on Ru-based catalysts.[17] These mechanistic findings provide a rigorous framework for the reactivity comparisons based on rate and equilibrium constants for elementary steps that are required for extension to other elements in their metal and sulfide forms and for connecting reactivity data with predictive molecular simulations on realistic cluster surfaces at near saturation sulfur coverages.

Results and Discussion

Thiophene HDS rates on supported Pt clusters

Dilution was used to avoid temperature or concentration gradients that can corrupt the kinetic origins of measured chemical reaction rates and selectivities and to ensure plug-flow hydrodynamics. Different extents of intrapellet (SiO_2/catalyst; 2–9) and bed dilution (quartz/catalyst = 200–400) did not influence measured thiophene turnover rates or product selectivities, confirming the absence of transport artifacts in measurements of turnover rates and selectivities.[28,29] Thiophene HDS turnover rates and selectivities were measured using thiophene-H_2 streams containing H_2S (0.3–5.0 kPa) to eliminate axial H_2S concentration gradients that would render rigorous kinetic analysis less definitive because of strong H_2S inhibition effects, even at low thiophene conversions.

Shown in Figure 1 a are thiophene conversion turnover rates at 573 K on Pt/SiO_2 (0.23 dispersion), as a function of residence time with different amounts of H_2S (0.5 to 1.0 and 2.0 kPa) present in the inlet thiophene-H_2 stream. At 0.5 kPa H_2S, thiophene conversion turnover rates decreased with increasing residence time (Figure 1 a), as a result of the combined kinetic effects of depletion of thiophene reactants (5–13 % conversion) and inhibition by product H_2S, whose concentration increases as thiophene conversion increases with residence time. Turnover rates decreased with increasing H_2S pressure (0.5 to 1.0 and 2.0 kPa, Figure 1 a), but the effects of residence time on turnover rates weakened concurrently, because of smaller axial changes in H_2S concentrations with increasing conversion at the higher inlet H_2S levels. All turnover rates herein are reported as the values extrapolated to zero residence time to exclude any kinetic effects of reactant depletion or product inhibition and to rigorously reflect the inlet concentrations of all relevant species.

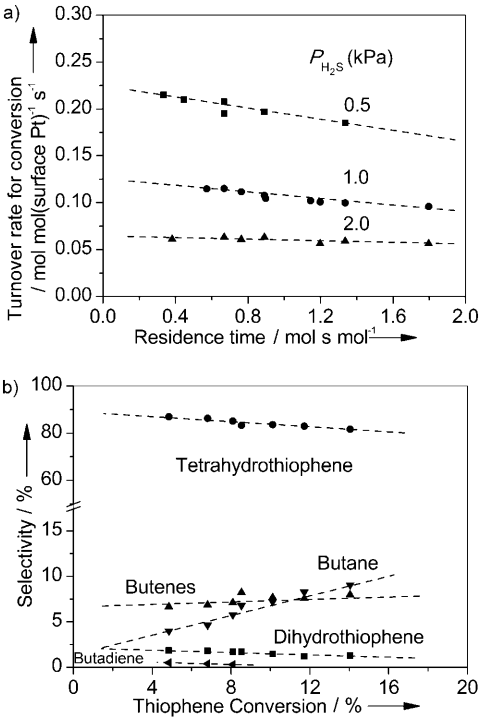

Figure 1. Total thiophene conversion turnover rates a) as a function of residence time (the reciprocal of the space velocity) on Pt/SiO_2 (0.23 dispersion) at 573 K, 2.5 kPa thiophene, 3.0 MPa H_2, and 0.5 kPa (■), 1.0 kPa (●), or 2 kPa H_2S (▲) and product selectivities b) as a function of thiophene conversion at 1.0 kPa H_2S.

Shown in Figure 1 b are the selectivities for thiophene reactions on Pt/SiO_2 (0.23 dispersion) at 573 K for reactant streams containing 1.0 kPa H_2S. Butadiene, 1-butene, *cis*-2-butene, *trans*-2-butene, *n*-butane, dihydrothiophene, and tetrahydrothiophene were detected in the effluent stream. 1-Butene, *cis*-

2-butene, and *trans*-2-butene were present as an equilibrated mixture at all conditions and on all catalysts; they are reported here as lumped species and denoted as butenes. No isomerization products of the alkanes and alkenes formed from thiophene or hydrogenolysis products of the decane molecules used as the internal standard and thiophene solvent were detected. Thiophene to tetrahydrothiophene ratios in the effluent approached a constant value (≈ 5.1 at 573 K and 3.0 MPa H_2) as thiophene conversions increased to above 40 %, because hydrogenation reactions approach equilibrium. Tetrahydrothiophene was the most abundant product at low conversions ($>$ 80 % selectivity; $<$ 15 % thiophene conversion; Figure 1 b), indicating that hydrogenation (HYD) is preferred over direct desulfurization (DS) routes on Pt-based catalysts at these conditions.

Butadiene, butenes, dihydrothiophene, and tetrahydrothiophene selectivities showed non-zero values when extrapolated to zero conversion (Figure 1 b), indicating that these molecules can form in a single surface sojourn and are therefore primary products. In contrast, *n*-butane forms through secondary hydrogenation reactions. Butadiene selectivities were small ($<$ 1 %) and became undetectable as thiophene conversion increased as a result of fast secondary hydrogenation reactions. Dihydrothiophene ($<$ 3 % selectivity) was also observed at low thiophene conversions, but underwent rapid subsequent hydrogenation to tetrahydrothiophene. Tetrahydrothiophene selectivity decreased with increasing thiophene conversion, because of its subsequent desulfurization to C_4 hydrocarbons and because thiophene hydrogenation approaches equilibrium, while the selectivity to *n*-butane, the final products of thiophene HDS reactions, concurrently increased. These residence time effects and product selectivities were similar for all Pt catalysts at all conditions examined.

These selectivity data are consistent with the sequence of primary and secondary reactions shown in Scheme 1, which we have shown recently to accurately describe all kinetic and isotopic data on Ru-based catalysts,[17] for which dihydrothiophene was too reactive to be detected. Thiophene HDS occurs on Pt clusters through two parallel pathways involving direct desulfurization (DS) to butadiene and *n*-butenes and sequential hydrogenation (HYD) to dihydrothiophene and then tetrahydrothiophene followed by sulfur removal. Secondary hydrogenation of butadiene, butenes, and dihydrothiophene and hydrogenation-desulfurization of tetrahydrothiophene lead to *n*-butane as the final product. DS and HYD turnover rates are reported separately and estimated by using total turnover rates and the initial selectivities to dihydrothiophene and tetrahydrothiophene (HYD) as well as butadiene and butenes (DS) calculated by extrapolation to zero thiophene conversion.

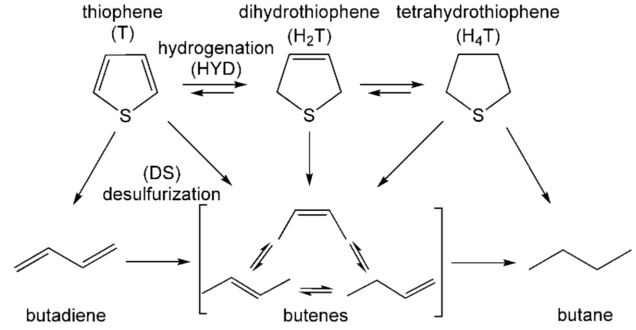

Scheme 1. Proposed thiophene hydrodesulfurization reaction network on Pt/SiO_2.

The kinetic response of DS and HYD turnover rates to thiophene, H_2, and H_2S concentrations is shown by the data in Figure 2 for Pt/SiO_2 (0.23 dispersion) at 573 K; other Pt catalysts showed a similar kinetic response. Shown in Figure 2 a,b is the effect of H_2 pressure on thiophene DS and HYD turnover rates at two H_2S/H_2 inlet ratios (a: 2×10^{-4} and b: 1×10^{-3}) and 2.5 kPa thiophene. At both H_2S/H_2 inlet ratios, DS and HYD turnover rates increased sublinearly with increasing H_2 pressure (2.0–2.5 times as the H_2 pressure increased from 1.0 to 3.0 MPa). The effects of H_2 pressure were slightly stronger at higher H_2S/H_2 ratios, apparently because of higher sulfur chemical potential and concentration of chemisorbed sulfur species. Similarly, DS and HYD turnover rates increased sub-linearly with increasing thiophene pressure (1–10 kPa) at both H_2S/H_2 ratios. The similar effects of H_2 and thiophene pressures on DS and HYD turnover rates are evident from the constant ratios of these rates over 3-fold and 10-fold changes in the pressure of H_2 and thiophene (Figure 2), respectively. These data suggest that DS and HYD reactions require similar site structures for the stabilization of the reactive intermediates involved in the kinetically relevant elementary steps, as also shown on Ru-based catalysts,[17] in contrast with the proposal for different sites for HYD and DS routes on MoS_2-based catalysts.[1,6,9,10]

Thiophene DS and HYD rates decreased strongly with increasing H_2S pressure (Figure 3 a,b), consistent with strong competitive adsorption of H_2S-derived species on surface sites also required for HYD and DS turnovers, as also shown on other catalysts.[1,7,17] At 3.0 MPa H_2, HYD turnover rates decreased from 0.20 to 0.022 mol mol(surface Pt)$^{-1}$ s^{-1} as the H_2S/H_2 inlet ratios increased from 0.10×10^{-3} to 1.67×10^{-3} (Figure 3 a). The effects of H_2S on DS turnover rates were even stronger; DS rates decreased from 0.028 to 0.0012 mol mol(surface Pt)$^{-1}$ s^{-1} as increasing H_2S pressures from 0.3 to 5.0 kPa (Figure 3 a). These weaker effects of H_2S on HYD compared with DS reflect the different types of H-species involved in their respective kinetically relevant steps.[17] H_2S dissociation forms protons, which react in the kinetically relevant steps for HYD, but not DS reactions. As a result, a term containing H_2S pressures appears in the numerator of the rate equation for HYD, but not DS, as shown in the next section and in previous studies of the elementary steps for these two routes on Ru-based catalysts.[17] This leads to the observed increase in HYD/DS ratios with increasing H_2S pressure and to their insensitivity to H_2 and thiophene pressures (for a given H_2S/H_2 ratio).

These kinetic effects of H_2, thiophene, and H_2S pressures on HYD and DS turnover rates resemble those observed on supported Ru clusters[17] and NiMo sulfides,[7] suggesting that these reactions share common elementary steps and reactive intermediates on all three active catalysts. In what follows, we propose a set of elementary steps consistent with these kinetic

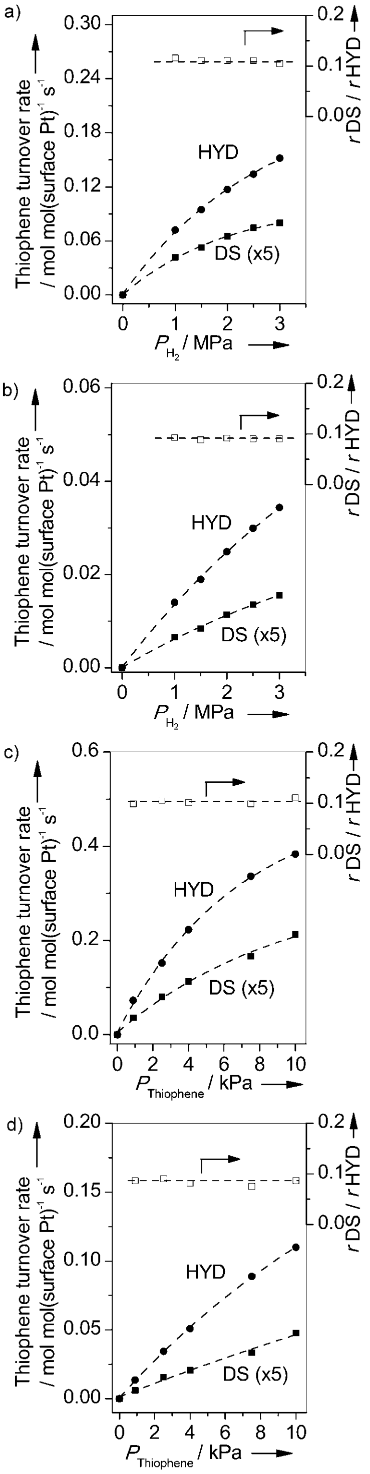

Figure 2. Effects of H_2 pressure at a) 2.5 kPa thiophene, a fixed H_2S to H_2 ratio of 2.0×10^{-4}, and b) 2.5 kPa thiophene, a fixed H_2S to H_2 ratio of 1.0×10^{-3} and thiophene pressure at c) 3.0 MPa H_2, a fixed H_2S to H_2 ratio of 2.0×10^{-4}, and d) 3.0 MPa H_2, a fixed H_2S to H_2 ratio of 1.0×10^{-3} on thiophene desulfurization (DS ■), hydrogenation (HYD ●) turnover rates, and their ratios (□) on Pt/SiO$_2$ (0.23 dispersion) at 573 K.

data and with the results of kinetic isotope effects and H_2–D_2 exchange measurements.

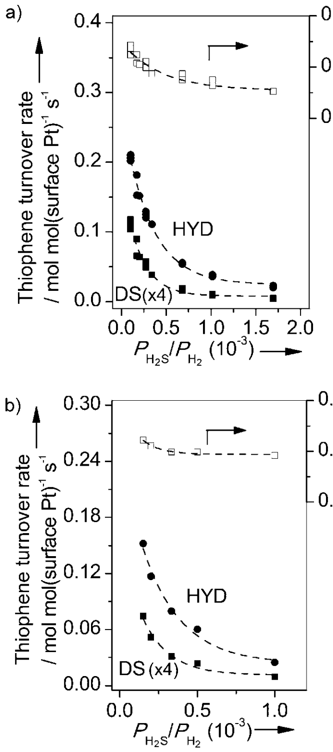

Figure 3. Effect of inlet H_2S/H_2 ratio on thiophene desulfurization (DS ■), hydrogenation (HYD ●) turnover rates, and their ratios (□) on Pt/SiO$_2$ (0.23 dispersion) at 573 K at a) 3.0 MPa H_2, 2.5 kPa thiophene and b) 2.0 MPa H_2, 2.5 kPa thiophene.

Elementary steps involved in HYD and DS reactions of thiophene on Pt clusters

Isolated sulfur vacancies with vicinal sulfur anions have been implicated, as the active structures on Ru catalysts,[17] which expose surfaces nearly saturated with chemisorbed sulfur during steady-state HDS catalysis, as expected from their strong metal–sulfur bonds.[24,30] These conclusions were confirmed by temperature-programmed reduction (TPR), X-ray absorption spectroscopy (XAS), and rate data after treatment protocols designed to form metal or sulfide clusters before catalytic tests.[17] The observed kinetic effects of the H_2S/H_2 ratio and temperature and the demonstrated equilibrated nature of H_2 and H_2S dissociation elementary steps indicate that sulfur chemical potentials depend only on H_2S/H_2 ratio (and temperature) and not on the individual concentrations of reactants and products.[17] The surface concentrations of vacancies and sulfur atoms during catalysis depend in turn on these sulfur chemical potentials and on the coordination number of exposed metal atoms, which vary with the size of the supported metal clusters.[17]

Pt surfaces bind sulfur atoms more weakly than Ru surfaces[24,30,31] and the heat of adsorption ($-\Delta H_{ads}$, [Eq. (1)]) of S-atoms is much smaller on Pt/Al$_2$O$_3$ (0.09 dispersion; 120 kJ mol^{-1}) than on Ru/Al$_2$O$_3$ (0.34 dispersion; 213 kJ mol^{-1}) at similar sulfur coverages ($\approx$0.7, fractional coverage based on Pt and Ru dispersion values).[30,31] The free energy (ΔG^0_{ads}) for sulfur adsorption:

$$Pt + H_2S \leftrightarrow Pt{-}S\ (surface) + H_2 \qquad \Delta G^0_{ads} = RT\ln(P_{H_2S}/P_{H_2}) \tag{1}$$

was estimated from the adsorption enthalpy and entropy on Pt/Al_2O_3 (0.09 dispersion).[31] This ΔG^0_{ads} value is $-60.4\ kJ\,mol^{-1}$ (at 573 K) and indicates that H_2S/H_2 ratios of around 3×10^{-6} are required for fractional sulfur coverage of 0.7. These ratios are much smaller than used in our study or of those typical of industrial practice (1×10^{-4} to 1.7×10^{-3}), indicating that sulfur coverage are near saturation on Pt clusters during catalysis. ΔG^0_f for the formation of bulk Pt sulfide (PtS) at 600 K is $-26.4\ kJ\,mol^{-1}$[24] and corresponds to a H_2S/H_2 ratio of 5×10^{-3}, which is larger than those prevalent in our study or in catalytic practice, indicating that the interior of Pt clusters remains metallic during HDS catalysis.

We consider here the involvement of site pairs consisting of an isolated vacancy (#) and a sulfur anion ($\#{-}S^{\delta-}$) in thiophene DS and HYD reactions on Pt metal surfaces with chemisorbed sulfur atoms at near saturation coverage. These sites resemble those required to catalyze these reactions on Ru surfaces (Section 3.1 of Ref [17]), which show similar kinetic behavior as the Pt clusters in the current study. The elementary steps in Scheme 2 are similar to those proposed for Ru-based catalysts[17] and are consistent with all previous kinetic and isotopic data.

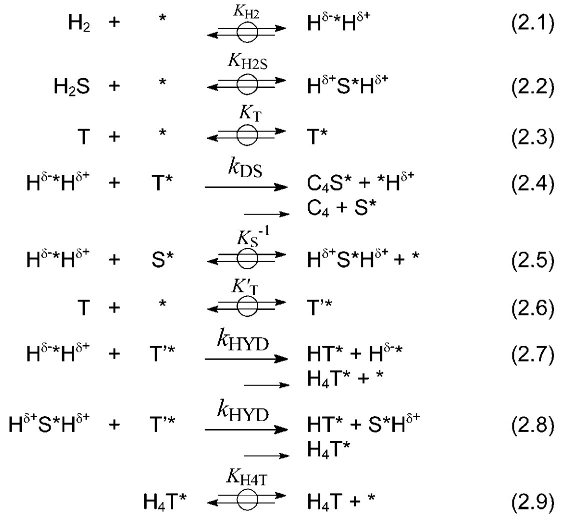

Scheme 2. Proposed reaction pathways for thiophene hydrodesulfurization on supported Pt metal clusters. (* is a vacancy-sulfur site-pair, #–#S; $\xleftrightarrow{\ominus}$ denotes a quasi-equilibrated step; T, T*, and T'* represent thiophene, η^1(S)-coordinated thiophene, and η^4-coordinated thiophene; H_4T represents tetrahydrothiophene; k_x and K_x are the kinetic and equilibrium constants, respectively, for individual elementary steps).

This sequence of steps includes quasi-equilibrated heterolytic dissociation of H_2 to form $H^{\delta-}$ and $H^{\delta+}$ (as -S–$H^{\delta+}$) species and of H_2S to form -S–$H^{\delta+}$ (on vacancies) and $H^{\delta+}$ (on sulfur anions; as -S–$H^{\delta+}$) [Steps (2.1) and (2.2), Scheme 2]. Thiophene binds onto sulfur vacancies by σ-bonding through the lone pair in the S-atom [η^1(S); Step (2.3)] or by π-bonding with the aromatic ring [η^4; Step (2.6)]. Subsequent reactions of $H^{\delta-}$ with η^1(S)-coordinated thiophene form an adsorbed thiolate that leads to DS products; reactions of -S–$H^{\delta+}$ with η^4-thiophene form protonated species as the first step in thiophene HYD [Steps (2.4), (2.7), (2.8)]. These steps are irreversible and represent the respective kinetically relevant steps in DS and HYD routes in thiophene HDS. The sulfur atoms formed in these steps then react with chemisorbed hydrogen atoms to form H_2S [Step (2.5)] by means of quasi-equilibrated H_2S and H_2 dissociation-recombination steps that re-form equilibrium concentrations of vacancy sites. When H_2S is present in reacting streams, $H^{\delta+}$ species can form through heterolytic dissociation of either H_2 [Step (2.1)] or H_2S [Step (2.2)]. As a result, H_2S can be used as a source of the protons required for HYD routes, but not DS routes, causing HYD reactions to be less strongly inhibited by H_2S than parallel DS reactions (Figure 3).

A pseudo-steady-state treatment for the intermediates and elementary steps in Scheme 2 leads to Equation (3) for DS and Equation (4) for HYD turnover rates in terms of H_2, thiophene, and H_2S pressures (P_j) and the rate or equilibrium constants for the relevant elementary steps.

$$r_{DS} = \frac{k_{DS}K_TP_TK_{H_2}P_{H_2}}{\alpha^2} \tag{3}$$

$$r_{HYD} = \frac{k_{HYD}K'_TP_T(K_{H_2}P_{H_2}+K_{H_2S}P_{H_2S})}{\alpha^2} \tag{4}$$

The derivation details are included in the supporting information. Each term in the common denominator (α) of these two equations represents the concentration of an intermediate relative to the concentration of sulfur vacancies; this denominator is given by Equation (5):

$$\alpha = \underset{\substack{\uparrow\\ *}}{1} + \underset{\substack{\uparrow\\ T^*}}{K_TP_T} + \underset{\substack{\uparrow\\ T'^*}}{K'_TP_T} + \underset{\substack{\uparrow\\ H^*H}}{K_{H_2}P_{H_2}} + \underset{\substack{\uparrow\\ HS^*H}}{K_{H_2S}P_{H_2S}} + \underset{\substack{\uparrow\\ S^*}}{K_S\frac{K_{H_2S}P_{H_2S}}{K_{H_2}P_{H_2}}} \tag{5}$$

The specific assignment of each denominator term to the intermediates in the elementary steps of Scheme 2 is shown immediately below Equation (5).

Equations (3)–(5) accurately describe measured thiophene DS and HYD rate data over a 50-fold range of turnover rates (Figure 4). Rate and equilibrium constants were derived from a regression analysis of measured rate data on Pt/SiO_2 (0.23 dispersion) at 573 K and these values are shown in Table 1. H_2S and thiophene show much larger equilibrium constants than H_2, as expected from the strong binding of sulfur-containing compounds on metal cluster surfaces and as also reported on Ru,[17] MoS_2,[1] and $NiMoS_x$ catalysts.[1,7] The relative values of these equilibrium constants show that S* species are much more abundant than HS*H species at the conditions of these experiments, in agreement with the proposal that dissociation

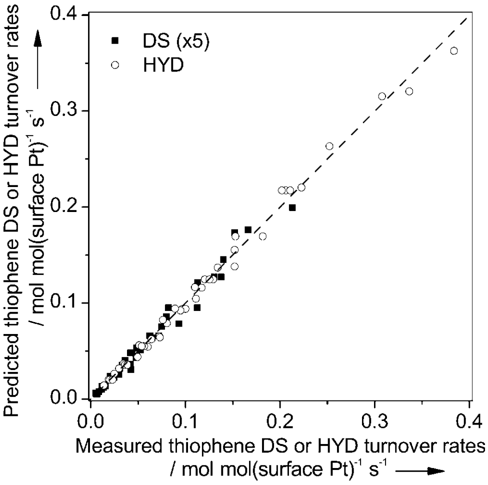

Figure 4. Parity plots of predicted (from Equations (3) and (4) and kinetic parameters in Table 1 for Pt/SiO_2 catalyst with 0.23 dispersion at 573 K) and measured thiophene desulfurization (■) and hydrogenation (○) turnover rates.

Table 1. Kinetic parameters estimated for thiophene hydrodesulfurzation (Pt/SiO_2 with 0.23 dispersion, 573 K, thiophene pressure range of 1.0–10.0 kPa, H_2 pressure range of 1.0–3.0 MPa, H_2S/H_2 ratio range of 0.1–3.0 × 10^{-3}).

Kinetic parameters[a]	Estimated values
$k_{DS}K_T$ (mol mol^{-1} s^{-1} kPa^{-1})	0.12 (±0.03)
$k_{HYD}K'_T$ (mol mol^{-1} s^{-1} kPa^{-1})	1.0 (±0.2)
$K_T+K'_T$ (kPa^{-1})	0.11 (±0.02)
K_{H_2} (kPa^{-1})	1.3 (±0.6) × 10^{-4}
K_{H_2S} (kPa^{-1})	8.7 (±6.0) × 10^{-2}
$K_S\ K_{H_2S}/K_{H_2}$	4.5 (±0.9) × 10^{3}

[a] For rate and equilibrium constants in Scheme 2 and Equations (3)–(5).

of H_2S on metals mainly forms S* via SH surface species as intermediates.[32] As a results, inhibition by H_2S reflects the occupancy of vacancies by S* and depends on H_2S/H_2 ratios [S* in Equation (5)] and is independent of H_2 [H*H in Equation (5)] or H_2S [HS*H in Equation (5)] pressures. Turnover rates are limited by the only two irreversible steps in Scheme 2: H-assisted C–S bond cleavage [Step (2.4); k_{DS}] and H-addition reactions [Step (2.7) or (2.8); k_{HYD}] for thiophene desulfurization and hydrogenation, respectively, consistent with the isotopic data reported in the next section. The mechanistic findings and catalytic consequences reported here for Pt are similar to those reported on Ru-based catalysts[17] and indicate that similar site requirements and elementary steps are likely to mediate desulfurization and hydrogenation on other metals similar in metal–sulfur bonds and surface reactivity to Ru and Pt.

Isotopic evidence for reversible H_2 and H_2S dissociation and kinetic isotope effects for DS and HYD reactions

The reversibility of H_2 and H_2S dissociative adsorption steps was probed by measuring the rate of formation of HD and $H_{2-x}D_xS$ isotopomers, respectively, during thiophene HDS reactions on Pt/SiO_2 (0.23 dispersion, 2.5 kPa thiophene, 573 K) using equimolar H_2/D_2 mixtures (3.0 MPa) containing H_2S (0.5 or 1.0 kPa).

The ratio of H_2/HD/D_2 isotopomers in the effluent stream was 1:2.0 ± 0.1:1.0 ± 0.1 at all thiophene conversions (2–15 %), consistent with binomial isotopic distributions (1:2:1) for equimolar mixtures and with the equilibration of hydrogen dissociation–recombination steps during steady-state thiophene HDS catalysis. Significant amounts of DHS and D_2S were also detected, even at low thiophene conversion. The H_2S/DHS/D_2S ratios were 1:2.0 ± 0.5:1.1 ± 0.4, consistent with the full isotopic equilibration of hydrogen sulfide molecules with the prevailing dihydrogen pool (H_2/HD/D_2 = 1:2.0 ± 0.1:1.0 ± 0.1) at all reaction conditions. The complete isotopic (and therefore chemical) equilibration between H_2 and H_2S indicates that the dissociative adsorption of H_2 and H_2S and the recombinative desorption of its surface fragments are in quasi-equilibrium during thiophene-H_2 reactions on Pt clusters, as assumed in the derivation of the rate equations[17] from the elementary steps in Scheme 2.

Kinetic isotope effects (r_H/r_D) were determined from thiophene DS and HYD turnover rates (extrapolated to zero residence time) measured with H_2-thiophene-C_4H_4S, D_2-thiophene-C_4H_4S, and D_2-thiophene-C_4D_4S reactant mixtures (2.0 and 3.0 MPa of H_2 or D_2, 20 and 2.5 kPa of thiophene, at $H_2S/H_2(D_2) = 5.0 \times 10^{-5}$) at 573 K on Pt/SiO_2 (0.23 dispersion). The measured kinetic isotope effects (KIE) are shown in Table 2. The presence of deuterium within thiophene did not lead to detectable kinetic effects, consistent with the similar equilibrium constants (K_T and K'_T) expected for molecular adsorption of [D_0] and [D_4] isotopologues of thiophene. H_2/D_2 kinetic isotope effects near unity (1.0–1.1) were observed for thiophene DS and HYD rates at all conditions tested, as also found on Ru catalysts (1.0 (DS) and 1.2 (HYD) KIE at 623 K, 3.0 MPa H_2, 2.5 kPa thiophene, 0 kPa H_2S; Ru/SiO_2, 0.58 dispersion).[17]

The H/D kinetic isotope effects for DS and HYD reactions are given by the ratios of the rate equations Equations (3) and (4)

Table 2. Measured kinetic isotope effects (KIE, r_H/r_D) for thiophene desulfurization (DS) and hydrogenation (HYD) on Pt/SiO_2 with 0.23 dispersion at 573 K and calculated kinetic isotope effect for surface reactions (k_H/k_D).

	Reactants			Measured KIE (r_H/r_D)[a]		Calculated KIE for kinetically relevant step (k_H/k_D)[b]	
	H_2 [MPa]	Thiophene [kPa]	H_2S [kPa]	DS	HYD	DS	HYD
(H_2/D_2)–C_4H_4S	3.0	20.0	0.15	1.0	1.1	1.5	1.6
(H_2/D_2)–C_4H_4S	2.0	20.0	0.10	1.0	1.1	1.5	1.6
(H_2/D_2)–C_4H_4S	3.0	2.5	0.15	0.9	1.1	–	–
D_2–(C_4H_4S/C_4D_4S)	3.0	2.5	0.15	1.0	1.0	–	–

[a] Ratio of rates for protium and deuterium forms of hydrogen or thiophene. [b] Ratio of rate constants [Steps (2.4), (2.7), and (2.8) in Scheme 2] for protium and deuterium forms of hydrogen or thiophene.

with undeuterated and deuterated forms of the reactants (see the Supporting Information). At the conditions of these isotopic measurements (20.0 kPa thiophene; 2.0 and 3.0 MPa H_2; a 5.0×10^{-5} H_2S/H_2 ratio), the adsorption constants estimated from rate data (Table 1) indicate that adsorbed thiophene ($K_TP_T+K_T'P_T$) and H_2 ($K_{H_2}P_{H_2}$) are the dominant species on vacancies (Supporting Information). In this case, the terms other than thiophene and H_2 can be neglected and the H/D kinetic isotope effects are given by Equations (6) and (7):

In which equilibrium constants (K_T and K_T') for molecular adsorption of d_0 and d_4 isotopologues of thiophene are similar. Measured rates reflect isotope effects from both equilibrium (K_{H_2}/K_{D_2}) and kinetic ($k_{DS,H}/k_{DS,D}$ or $k_{HYD,H}/k_{HYD,D}$) origins.

$$KIE_{DS}=\frac{r_{DS,H}}{r_{DS,D}}=\frac{k_{DS,H}K_{H_2}}{k_{DS,D}K_{D_2}}\times\left(\frac{1+K_TP_T+K_T'P_T+K_{D_2}P_{D_2}}{1+K_TP_T+K_T'P_T+K_{H_2}P_{H_2}}\right)^2 \tag{6}$$

$$KIE_{HYD}=\frac{r_{HYD,H}}{r_{HYD,D}}=\frac{k_{HYD,H}K_{H_2}}{k_{HYD,D}K_{D_2}}\times\left(\frac{1+K_TP_T+K_T'P_T+K_{D_2}P_{D_2}}{1+K_TP_T+K_T'P_T+K_{H_2}P_{H_2}}\right)^2 \tag{7}$$

Equilibrium isotope effects for dissociative H_2 adsorption (K_{H_2}/K_{D_2}) are smaller than unity, because D* binds more strongly than H* on metal surfaces and subsequently the differential zero-point energy value (H* or D* to H–H or D–D) is greater with H_2 than D_2 dissociation.[33,34,35] Theoretical estimates[33] show an inverse thermodynamic isotope effect for dissociative adsorption of H_2/D_2 (≈ 0.61 at 508 K) on Fe and Co surfaces saturated with chemisorbed CO. Our experimental measurement of H_2 and D_2 adsorption isotherms on SiO_2 supported Pt (3.6 nm) at 623 K and low hydrogen coverages gives values of 0.66 ± 0.02.[35] Measurements of these thermodynamic H_2/D_2 isotope effects on sulfur-saturated metal surfaces are neither available nor feasible. As a result, we assume that sulfur covered surfaces exhibit isotope effects similar to those measured on Pt surfaces at low hydrogen coverages ($K_{H_2}/K_{D_2}=0.66$)[35] for H_2 dissociation on Pt and take the equilibrium constants for thiophene adsorption to be independent of isotopic identity, as mentioned above. These values, taken together with Equations (6) and (7) and measured kinetic isotope effects for DS and HYD reactions, give normal KIE values for the kinetically relevant elementary steps for both DS and HYD routes [$k_{DS,H}/k_{DS,D}=1.5$ for DS, Step (2.4); $k_{HYD,H}/k_{HYD,D}=1.6$ for HYD Step (2.7); Table 2]. These small normal isotope effects are consistent with the proposed surface reaction mechanisms in Scheme 2, in which hydrogen-derived species in C–S bond cleavage and hydrogen addition reactions control DS and HYD rates, respectively. As proposed previously,[17] these surface reactions involve reactant-like transition states, and hence the zero-point energy differences between H- and D-containing transition states are slightly lower than those for the ground. Therefore, the contributions from zero-point energy to the activation energy will be small, leading to a normal but small KIE values.[36]

Effects of Pt cluster size and metal identity on thiophene HDS turnover rates

HYD and DS turnover rates decreased markedly with increasing Ru dispersion.[17] These trends reflect the stronger binding of sulfur atoms on coordinatively unsaturated surface atoms at corners and edges, which prevail on small metal clusters.[37] Similar effects of metal cluster size on turnover rates have been reported on surfaces nearly saturated with chemisorbed oxygen atoms for oxidation reactions of dimethyl ether,[38] methane,[39] and NO[26,27] on supported Pt clusters; these reactions share the common requirement of vacancies on heteroatom-covered surfaces for their respective kinetically relevant steps, the surface density of which is much lower on coordinatively unsaturated surfaces. We show here that similar effects of cluster size and mechanistic interpretations are applicable to HDS reactions on Pt clusters.

HYD and DS turnover rates increased with increasing metal cluster size on Pt/SiO_2 catalysts (0.13–0.81 dispersion, 1.4–8.4 nm mean cluster diameter) (Figure 5). These effects were observed at H_2S pressures of 0.5 kPa ($H_2S/H_2=1.7\times10^{-4}$; Figure 5 a) and 2.0 kPa ($H_2S/H_2=6.7\times10^{-4}$; Figure 5 b). These strong effects of cluster size on thiophene DS and HYD turnover rates at both sulfur chemical potentials are consistent with the higher intrinsic reactivity of low-index planes with more coordinatively saturated exposed Pt atoms, which bind S-atoms more weakly than the corner and edge sites more abundant on smaller clusters. The inhibition effects of H_2S on DS and HYD reactions were stronger on the smaller Pt clusters (Figure 5 c), also consistent with the stronger binding of sulfur on coordinatively unsaturated Pt atoms. These effects of surface coordination on sulfur binding control the surface density of vacancies available for kinetically relevant steps at any given sulfur chemical potential in the reacting stream. These sulfur vacancies are required for dissociation of H_2 and H_2S and for thiophene adsorption to form the adsorbed species involved in the kinetically relevant steps for DS and HYD reactions.

The ratio of DS to HYD turnover rates increased with decreasing Ru cluster size (Figure 5 d) indicating that these two pathways sense the coordinative unsaturation of exposed atoms differently, even though both require sulfur vacancies in their respective kinetically relevant steps. These data suggest that larger clusters, with lower sulfur coverages and flatter exposed surfaces, favor the η^4-coordination mode required in HYD routes [Step (2.6), Scheme 2] over the $\eta^1(S)$-coordination mode required in DS routes [Step (2.3)]. Thermal desorption spectroscopy studies of the adsorption and reaction of thiophene on Mo surface have shown that the orientation of thiophene with respect to metal surfaces is sensitive to the coverage of coadsorbed species.[40–42] A parallel geometry is favored at low coverages and more perpendicular orientations of the ring prevail high coverage, apparently as a result of steric repulsion.[40–42] As a result, the extent to which thiophene is consumed through DS pathways mediated by $\eta^1(S)$-intermediates is greater on smaller clusters. These proposals about the effects of sulfur coverage and packing density on thiophene coordination are consistent with previous theoretical evidence

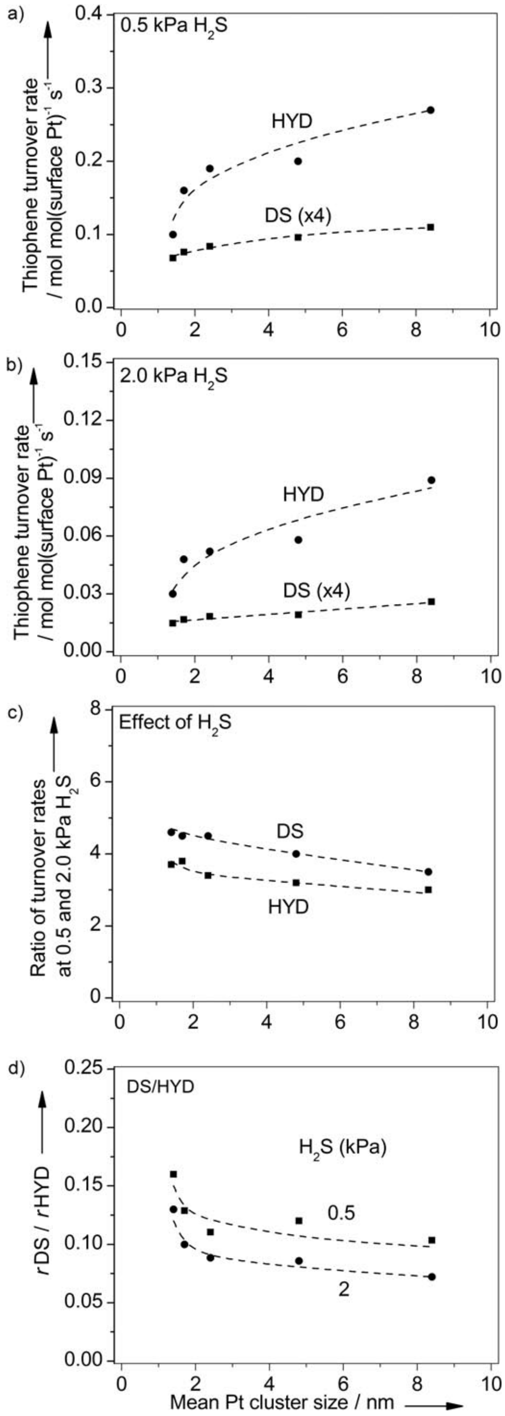

Figure 5. Effect of mean Pt cluster size on a) thiophene desulfurization and hydrogenation turnover rates at 0.5 kPa H_2S (H_2S to H_2 ratio of 0.17×10^{-4}); b) thiophene desulfurization and hydrogenation turnover rates at 2 kPa H_2S (H_2S to H_2 ratio of 6.67×10^{-4}); c) ratio of turnover rates at 0.5 kPa H_2S and 2 kPa H_2S for desulfurization (DS) and hydrogenation (HYD); and d) ratios of turnover rates for desulfurization and hydrogenation over Pt/SiO_2 catalysts (573 K, 3.0 MPa H_2, 2.5 kPa thiophene).

for η^1(S) structures that become preferred over η^4-coordination on exposed Ni atoms on NiS_x clusters as the sulfur coverage increases.[11]

The catalytic consequences of Pt cluster size reported here are similar for Ru-based catalysts[17] and indicate that the elementary steps in Scheme 2 and their implications for rates and selectivities are general for noble metal HDS catalysts and are likely to also account for the similar, but less conclusive, effects of reaction conditions, cluster size, support, and coordination on more complex MoS_x systems and their Co and Ni promoters.

We consider next the reactivity and selectivity of Pt and Ru clusters of a given size in the context of the mechanistic details in Scheme 2. Thiophene HYD turnover rates on Pt clusters (8.4 nm) were about 30 times larger than on Ru clusters of similar size (6.2 nm) and DS turnover rates were about 5 times higher at 573 K and 0.5 or 2 kPa H_2S (Table 3). H_2S inhibition effects on DS and HYD reactions were weaker on Pt than on Ru clusters (Table 3). These differences indicate that Pt cluster surfaces, which bind sulfur more weakly than Ru surfaces[24,30,31,43] exhibit larger numbers of vacancy sites, which are required for the kinetically relevant steps in Scheme 2. The heat of adsorption ($-\Delta H_{ads}$) of sulfur on Pt/Al_2O_3 (5 wt.%, 0.09 dispersion) is about 93 $kJ\,mol^{-1}$ lower than Ru/Al_2O_3 (1.5 wt.%, 0.34 dispersion) at the same sulfur coverage of ≈0.7.[30,31,43] Similar effects of metal identity and interpretations based on heteroatom binding energies were reported for dimethyl ether[25] and NO oxidation;[26,27] in these studies, Pt gave higher turnover rates than Pd or Rh because it binds oxygen more weakly and exposes surfaces with a greater density of vacancies during steady-state catalysis.[25] The higher HYD selectivity observed on Pt at all conditions (Table 3) also reflects a lower sulfur coverage, which in turn leads to a preference for η^4 thiophene adsorption over η^1(S) adsorption.

The effects of crystallite size and metal identity on turnover rates reflect predominantly the effects of sulfur binding energy on metal clusters with surfaces nearly saturated with sulfur and the concomitant availability of vacancy sites required for the kinetically relevant steps in DS and HYD pathways for sulfur removal. Metal–sulfur bonds are weaker on Pt than on Ru and on low-index planes than on coordinatively unsaturated corner and edge surface atoms. These conclusions are based on rigorous comparisons of surface reactivity on clusters that remain metallic during HDS at practical conditions and which catalyze HYD and DS sulfur removal pathways by means of analogous mechanisms and on a single type of active site. The preeminence of metal–sulfur bond energies as a determinant of reactivity is in agreement with previous proposals based on monotonic trends in catalytic productivity with metal–sulfur bond energies in bulk sulfides for materials with different cluster size and present as either metals or sulfides during steady-state catalysis.[1,8,18,19] The kinetic and isotopic data shown here provide rigorous evidence for the origins of reactivity on clusters of noble metals that remain metallic during catalysis, but with surfaces saturated with sulfur at conditions relevant to hydrodesulfurization catalysis. The concentration of vacancies required for HYD and DS pathways depends on the sulfur chemical potential in the reactant stream, which is set by temperature and H_2S/H_2 ratio, and the ability of exposed atoms, because of their identity and coordination, to

Table 3. Thiophene desulfurization and hydrogenation turnover rates, inhibition effect of H_2S, and pathway selectivities over Pt/SiO_2 catalyst (0.3 wt.%, 8.4 nm) and Ru/SiO_2 catalyst (1.0 wt.%, 6.2 nm) at 573 K.

Catalyst	P_{H_2S} [kPa]	Turnover rate [$\times 10^{-2}$][a]		Selectivity (r_{DS}/r_{HYD})[b]	Ratio of rates at 0.5 and 2 kPa H_2S[c]	
		DS	HYD		DS	HYD
Pt/SiO_2	0.5	2.6	27	0.097	4.0	3.0
	2.0	0.65	8.9	0.073		
Ru/SiO_2	0.5	0.56	0.92	0.61	4.7	3.7
	2.0	0.12	0.25	0.48		

[a] mol(mol surface Pt)$^{-1}$ s^{-1}, extrapolated to zero residence time and conversion (573 K, 3.0 MPa of H_2, 2.5 kPa of thiophene). [b] Ratio of turnover rates for desulfurization (DS) and hydrogenation (HYD). [c] Ratio of turnover rates at 0.5 kPa H_2S and 2 kPa H_2S for desulfurization (DS) and hydrogenation (HYD).

bind sulfur atoms involved as intermediates in the elementary steps that provide a catalytic sequence for hydrodesulfurization.

Conclusions

Kinetic and isotopic measurements of thiophene hydrodesulfurization on dispersed Pt clusters are consistent with kinetically relevant steps involved in parallel desulfurization and hydrogenation sulfur-removal pathways and the critical role of vacancies within sulfur-saturated cluster surfaces. Elementary steps involve equilibrated heterolytic H_2 and H_2S dissociation on vacancies and thiophene adsorption in η^1(S) or η^4 coordination on vacancies, consistent with the measured effects of H_2, H_2S, and thiophene concentrations on turnover rates and with the isotopic evidences. Hydrogenation proceeds via proton addition to η^4-thiophene, whereas desulfurization involves C–S activation in η^1(S)-thiophene aided by hydride species formed via H_2 dissociation. These two steps limit the reaction turnover rates, consistent with the measured H_2/D_2 kinetic isotope effects. Desulfurization and hydrogenation routes require similar sulfur vacancy sites present on Pt surfaces nearly saturated with sulfur during steady-state catalysis. Turnover rates are lower and inhibition by H_2S is stronger on smaller Pt clusters for both hydrogenation and desulfurization because of the stronger binding of sulfur and lower vacancy densities on surface atoms with lower coordination prevalent on small clusters. Binding in η^1(S) configurations is preferred over η^4 binding at the higher S coverages prevalent on small clusters, and therefore the ratio of desulfurization and hydrogenation turnover rate decreases with increasing cluster size. Pt clusters give much higher turnover rates than Ru clusters of similar size because Pt–S bonds are significantly weaker than Ru–S bonds. We conclude that metal–sulfur bond energies depend on the identity and size of metal clusters and, together with temperature and H_2S/H_2 ratios, they control the density of vacancies and the reactivity of cluster surfaces in hydrodesulfurization catalysis. These mechanistic findings, cluster size effects, and catalytic consequences on Pt clusters resemble those on supported Ru clusters that we reported previously, suggesting that our conclusions apply generally to hydrodesulfurization on metals similar in metal–sulfur bonds and surface reactivity to Pt and Ru, and are expected to be relevant to more complex MoS_x systems and their Co and Ni promoters that require sulfur vacancies for hydrodesulfurization catalysis.

Experimental Section

Silica (Cabosil, HS-5, 310 m^2 g^{-1}) was treated in ambient air at 673 K (0.033 K s^{-1}) for 3 h before Pt deposition. SiO_2-supported Pt (Pt content of 0.3 wt.%) was prepared by means of strong electrostatic adsorption methods.[17,44] SiO_2 was added to an aqueous solution (pH 9.4, 200 cm^3 g^{-1} SiO_2) of $[Pt(NH_3)_4(NO_3)_2]$ (Alfa Aesar, 99.99 %; 7.7×10^{-6} mol cm^{-3} in the obtained solution) and $NH_3{\cdot}H_2O$ (Sigma–Aldrich) and stirred for 1 h (final pH 9.3) at ambient temperature. The solids were separated by filtering, kept in vacuum at ambient temperature for $>$24 h, and treated in flowing dry air (Praxair, 99.99 %, 1.0 cm^3 g^{-1} s^{-1}) at 373 K (0.033 K s^{-1}) 5 h. The sample was then treated in flowing dry air (Praxair, 99.99 %, 1.0 cm^3 g^{-1} s^{-1}) by increasing the temperature to 673–873 K at 0.05 K s^{-1} and holding for 5 h to prepare samples with a broad range of Pt fractional dispersion (0.13–0.81, measured by H_2 chemisorption as described below; Table S1 in the Supporting Information). These samples were then treated in 9 % H_2/He (Praxair, 1.67 cm^3 g^{-1} s^{-1}) at 673 K (0.033 K s^{-1}) for 1 h and passivated in 0.5 % O_2/He (Praxair, 0.05 cm^3 g^{-1} s^{-1}) at ambient temperature for 6 h before exposure to ambient air. Passivated samples were subsequently treated in situ in flowing H_2 (Praxair, 99.999 %, 50 cm^3 g^{-1} s^{-1}) by heating from ambient temperature to 673 K at 0.083 K s^{-1} and holding for 1 h before catalytic and dispersion measurements.

The Pt content in these samples was measured by using inductively coupled plasma-optical emission spectroscopy (ICP-OES; Galbraith laboratories). The fraction of the Pt atoms exposed at surfaces (Pt dispersion) was determined from uptakes of strongly chemisorbed hydrogen by using a Quantasorb chemisorption analyzer (Quantachrome Corp.). After treatment in flowing H_2 (Praxair, 99.999 %, 0.83 cm^3 g^{-1} s^{-1}) by heating to 673 K at 0.033 K s^{-1} and holding for 1 h and then in dynamic vacuum at 673 K for 1 h, H_2 uptakes were measured volumetrically at 313 K and 10–120 kPa H_2. The samples were then treated in dynamic vacuum at 313 K for 0.5 h and another H_2 adsorption isotherm was then measured. These two isotherms were extrapolated linearly to zero H_2 pressures and their difference was used to determine Pt dispersions by assuming a 1:1 H/Pt surface stoichiometry. Mean cluster diameters were estimated from these dispersion values by assuming hemispherical clusters and the density of bulk Pt metal (21.45 g cm^{-3}).[45] Pt dispersions and average cluster diameters are reported in Table S1 in supporting information for all samples.

Thiophene HDS turnover rates and product selectivities were measured in a continuous flow packed-bed tubular reactor with plug-flow hydrodynamics. Catalyst powders were diluted with SiO_2 (Cabosil, HS-5, 310 m^2 g^{-1}; 9:1 SiO_2/catalyst mass ratio) and the mixture was pressed and sieved to retain 0.125–0.18 mm aggregates. A portion of these diluted aggregates (containing 5–10 mg catalyst) were then loosely mixed with acid-washed quartz granules of the same size (Fluka, acid purified; 1.0 g) to avoid temperature or concentration gradients in the bed and pellet scales. The reactant stream contained thiophene (Alfa Aesar, 99%; 1–10 kPa), *n*-decane (Sigma–Aldrich, 99+%; 50 kPa, as the solvent for thiophene and internal standard), H_2S (0.5% H_2S/H_2, Praxair, certified mixture; 0.3–5 kPa H_2S), and H_2 (Praxair, 99.999%; 1.0–3.0 MPa). Reactant and product concentrations were measured by on-line gas chromatography (Agilent 6890) using a methyl silicone capillary column (HP-1, Agilent, 25 m×0.32 mm×0.52 μm) connected to a flame ionization detector and a Porapak Q packed column (Supelco, 1.82 m×3.18 mm, 80–100 mesh) connected to a thermal conductivity detector. Additional details of the catalytic rates and selectivities measurement have been described elsewhere.[17]

Isotopic exchange rates (H_2–D_2 and D_2–H_2S) and kinetic isotope effects (H_2–D_2, thiophene–C_4H_4S–C_4D_4S) were measured on a Pt/SiO_2 catalyst with 0.23 dispersion. Chemical and isotopic compositions were measured by using on-line mass spectrometry (Leybold Inficon, Transpector Series) and also off-line analysis by gas chromatography with mass-selective and flame ionization detection (Agilent 6890 GC-MS system). [D_4]Thiophene (Isotec, chemical purity > 99.0%), D_2 (Spectra Gases Inc., UHP), H_2 (Praxair, 99.999%), and H_2S/He (Praxair, certified mixture) were used as reagents. Detailed conditions for each experiment are described together with the corresponding data in previous sections.

Acknowledgements

This work was supported by the Director, Office of Basic Energy Sciences, Chemical Sciences Division of the US Department of Energy under Contract DE-AC02-05CH11231. The authors acknowledge Drs. David Flaherty, Zhijie Wu, Ms. Cathy Chin, and Mr. Brett Loveless of the University of California at Berkeley for their careful review of the contents and conclusions of this manuscript. The authors also thank Dr. Mónica García-Diéguez of the University of California at Berkeley for help with the measurement of H_2 and D_2 adsorption isotherms.

Keywords: cluster-size effect · hydrodesulfurization · kinetics · platinum · reaction mechanisms · thiophene

[1] H. Topsøe, B. S. Clausen, F. E. Massoth in *Catalysis Science and Technology, Vol. 11* (Eds.: J. R. Anderson, M. Boudart), Springer-Verlag, New York, **1996**, pp. 1–231.

[2] R. Prins, V. H. J. de Beer, G. A. Somorjai, *Catal. Rev. Sci. Eng.* **1989**, *31*, 1–41.

[3] D. D. Whitehurst, T. Isoda, I. Mochida, *Adv. Catal.* **1998**, *42*, 345–471.

[4] M. J. Girgis, B. C. Gates, *Ind. Eng. Chem. Res.* **1991**, *30*, 2021–2058.

[5] C. S. Song, *Catal. Today* **2003**, *86*, 211–263.

[6] S. Kasztelan, D. Guillaume, *Ind. Eng. Chem. Res.* **1994**, *33*, 203–210.

[7] A. Borgna, E. J. M. Hensen, J. A. R. can Veen, J. W. Niemantsverdriet, *J. Catal.* **2004**, *221*, 541–548.

[8] A. Daudin, S. Brunt, G. Perot, P. Raybaud and C. Bouchy, *J. Catal.* **2007**, *248*, 111.

[9] S. Helveg, J. V. Lauritsen, E. Lægsgaard, I. Stensgaard, J. K. Nørskov, B. S. Clausen, H. Topsøe, F. Besenbacher, *Phys. Rev. Lett.* **2000**, *84*, 951–954.

[10] J. V. Lauritsen, J. Kibsgaard, G. H. Olesen, P. G. Moses, B. Hinnemann, S. Helveg, J. K. Nørskov, B. S. Clausen, H. Topsøe, E. Lægsgaard, F. Besenbacher , *J. Catal.* **2007**, *249*, 220–233.

[11] M. Neurock, R. A. van Santen, *J. Am. Chem. Soc.* **1994**, *116*, 4427–4439.

[12] E. J. M. Hensen, P. J. Kooyman, T van der Meer, A. M. van der Kraan, V. H. J. de Beer, J. A. R. van Veen, R. A. van Santen, *J. Catal.* **2001**, *199*, 224–235.

[13] T. A. Pecoraro, R. R. Chianelli, *J. Catal.* **1981**, *67*, 430–445.

[14] M. Lacroix, N. Boutarfa, C. Guillard, M. Vrinat, M. Breysse, *J. Catal.* **1989**, *120*, 473–477.

[15] A. Niquille-Röthlisberger, R. Prins, *J. Catal.* **2006**, *242*, 207–216.

[16] A. Ishihara, F. Dumeignila, J. Lee, K. Mitsuhashi, E. W. Qian, T. Kabe, *Appl. Catal. A* **2005**, *289*, 163–173.

[17] H. Wang, E. Iglesia, *J. Catal.* **2010**, *270*, 245–256.

[18] H. Topsøe, B. S. Clausen, N. Y. Topsøe, J. Hyldtoft, J. K. Nørskov, *ACS Petrol. Div. Prepr.* **1993**, *38*, 638.

[19] J. K. Nørskov, B .S. Clausen, H Topsøe, *Catal. Lett.* **1992**, *13*, 1–8.

[20] R. R. Chianelli, *Catal. Rev. Sci. Eng.* **1984**, *26*, 361–393.

[21] E. J. M. Hensen, H. J. A. Brans, G. M. H. J. Lardinois, V. H. J. de beer, J. A. R. van Veen, R. A. van Santen, *J. Catal.* **2000**, *192*, 98–107.

[22] H. Toulhoat, P. Raybaud, *J. Catal.* **2003**, *213*, 63–72.

[23] N. Guernalec, C. Geantet, T. Cseri, M. Vrinat, H. Toulhoat, P. Raybaud, *Dalton Trans.* **2010**, *39*, 8420–8422.

[24] C. H. Bartholomew, P. K. Agrawal, J. R. Katzer, *Adv. Catal.* **1982**, *31*, 135–242.

[25] A. Ishikawa, E. Iglesia, *J. Catal.* **2007**, *252*, 49–56.

[26] B. M. Weiss, E. Iglesia, *J. Phys. Chem. C* **2009**, *113*, 13331–13340.

[27] B. M. Weiss, E. Iglesia, *J. Catal.* **2010**, *272*, 74–81.

[28] R. M. Koros, E. J. Nowak, *Chem. Eng. Sci.* **1967**, *22*, 470–493.

[29] R. J. Madon, M. Boudart, *Ind. Eng. Chem. Fundam.* **1982**, *21*, 438–447.

[30] J. G. McCarty, H. Wise, *J. Chem. Phys.* **1981**, *74*, 5877–5880.

[31] J. G. McCarty, K. M. Sancier, H. Wise, *J. Catal.* **1983**, *82*, 92–97.

[32] J. M. Saleh. C. Kemball, M. W. Roberts, *Trans. Faraday Soc.* **1961**, *57*, 1771–1780.

[33] M. Ojeda, A. Li, R. Nabar, A. U. Nilekar, M. Mavrikakis, E. Iglesia, *J. Phys. Chem. C* **2010**, *114*, 19761–19770.

[34] R. M. Bullock, B. R. Bender, *Isotope Methods—Homogeneous. In Encyclopedia of Catalysis* (Ed.: I. T. Horváth), Wiley, Hoboken, NJ, **2003**, pp. 1–62.

[35] H. Wang, M. García-Diéguez, E. Iglesia, unpublished results.

[36] F. H. Westheimer, *Chem. Rev.* **1961**, *61*, 265–273.

[37] R. van Hardeveld, F. Hartog, *Surf. Sci.* **1969**, *15*, 189–230.

[38] A. Ishikawa, M. Neurock, E. Iglesia, *J. Am. Chem. Soc.* **2007**, *129*, 13201–13212.

[39] C. Chin, E. Eglesia, unpublished results.

[40] B. C. Wiegand, C. M. Friend, *Chem. Rev.* **1992**, *92*, 491–504.

[41] F. Zaera, E. B. Kollin, J. L. Gland, *Surf. Sci.* **1987**, *184*, 75–89.

[42] D. G. Kelly, M. Salmeron, G. A. Somorjai, *Surf. Sci.* **1986**, *175*, 465–486.

[43] H. Wise, J. McCarty. J. Oudar in *Deactivation and poisoning of catalysts*, (Eds.: J. Oudar, H. Wise), Marcel Dekker Inc., New York, **1985**, pp. 1–50.

[44] J. T. Miller, M. Schreier, A. J. Kropf, J. R. Regalbuto, *J. Catal.* **2004**, *225*, 203–212.

[45] R. L. David, in *Handbook of Chemistry and Physics, 87th ed.* (Ed.: D. R. Lide), CRC Press, Boca Raton, Fl, **2006**, pp. 4–81.

Received: January 22, 2011